PERGAMON

International Journal of Solids and Structures 40 (2003) 6969–6980

INTERNATIONAL JOURNAL OF SOLIDS and STRUCTURES

www.elsevier.com/locate/ijsolstr

Kagome plate structures for actuation

R.G. Hutchinson [a], N. Wicks [b], A.G. Evans [c], N.A. Fleck [a], J.W. Hutchinson [b,*]

[a] *Engineering Department, Cambridge University, Cambridge, UK*
[b] *Division of Engineering and Applied Sciences, Harvard University, 29 Oxford Street Pierce Hall, Cambridge, MA 02138, USA*
[c] *Department of Materials Engineering, University of California, Santa Barbara, CA, USA*

Received 21 October 2002

Abstract

A class of planar, pin-jointed truss structures based on the ancient Kagome basket weave pattern with exceptional characteristics for actuation has been identified. Its in-plane stiffness is isotropic and has optimal weight among planar trusses for specified stiffness or strength. The version with welded joints resists plastic yielding and buckling, while storing minimal energy upon truss bending during actuation. Two plate structures are considered which employ the planar Kagome truss as the actuation plane. It is shown that these plates can be actuated with minimal internal resistance to achieve a wide range of shapes, while also sustaining large loads through their isotropic bending/stretching stiffness, and their excellent resistance to yielding/buckling.

Keywords: Trusses; Plates; Actuation; Buckling; Kagome

1. Introduction

A class of actuating plate structures is introduced, based on a planar truss having the Kagome weave pattern (Fig. 1). The two planar manifestations to be explored both consist of faces connected by a tetrahedral truss core (Fig. 2) with the following distinctions:

(i) A Kagome plane and a solid skin,
(ii) two Kagome faces.

The feature rendering the Kagome planar truss exceptional for actuation is that its members can be actuated (elongated or contacted) to achieve arbitrary in-plane nodal displacements with minimal internal resistance. This attribute arises because the infinite, pin-jointed version satisfies most of the requirements for static determinacy, permitting minimal elastic energy storage (in bending) even when the joints are welded. These benefits become apparent upon comparing with a highly redundant (isotropic) planar truss,

* Corresponding author. Tel.: +1-617-495-1000; fax: +1-609-258-1177.
E-mail address: hutchinson@husm.harvard.edu (J.W. Hutchinson).

0020-7683/$ - see front matter
doi:10.1016/S0020-7683(03)00348-2

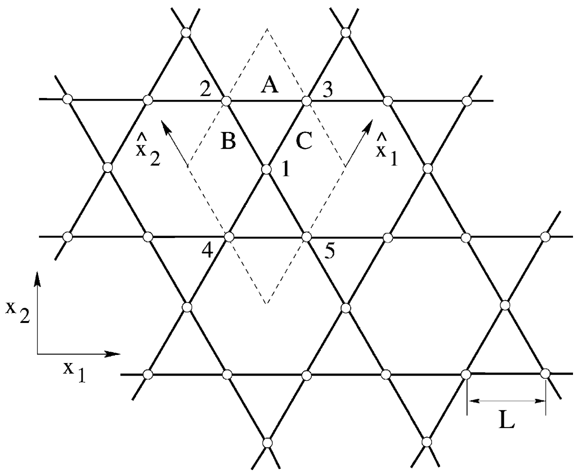

Fig. 1. Sketch of pin-jointed, planar Kagome lattice with member length L. Dashed lines give the boundaries of the primitive unit cell.

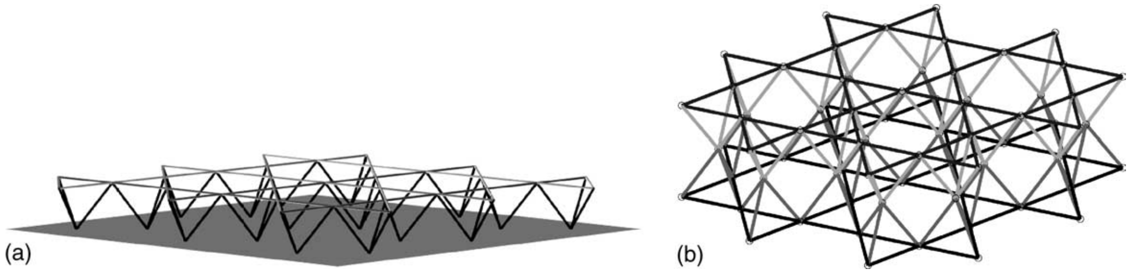

Fig. 2. Sandwich plates based on planar Kagome truss plates. (a) Sandwich with one Kagome truss face and a solid skin face and (b) sandwich with two Kagome truss faces.

exemplified by identical triangular units with equal length members. If such a truss replaces the Kagome in Fig. 2, axial deformation of the members would be required upon actuation, storing substantial energy. The Kagome truss is the only example known to us of an infinite planar truss amenable to assembly from repeat units having both isotropic stiffness and the properties desired for actuation.

The purpose of this paper is to introduce some important properties of the Kagome planar truss and to provide an overview of its role in actuating plate structures. More complete treatments will be given in subsequent papers. Several aspects of the performance of this configuration will be addressed.

(i) A discussion of determinacy for infinite pin-jointed trusses with repeating units reveals that no such configuration can be both statically and kinematically determinate.
(ii) The pin-jointed Kagome truss has kinematic mechanisms, but the weld-jointed version is resistant to premature failure by suppressing them and, moreover, inhibits premature failure by either plastic yielding or buckling.
(iii) In combination with superior in-plane stiffness (Hyun and Torquato, 2002), these features render the Kagome planar truss an ideal structural unit for two-dimensional actuation.
(iv) The actuation capability is revealed by analyzing the response of the plates in Fig. 2 at long wavelengths (relative to the truss member length).

2. Determinacy and the Kagome planar truss

The relevance of static determinacy to actuation of two- and three-dimensional truss structures has been appreciated for some time in connection with the design of space antenna and mirrors (Miura, 1984a,b; Rhodes and Mikulas, 1985; Mikulas et al., 1993). Because the forces in the members of a pin-jointed, statically determinate truss are determined by equilibrium alone, any member can be elongated or shortened without inducing forces in other members, at least to lowest order in the nodal displacements. Accordingly, the structure offers no resistance to actuation, yet, simultaneously, it is capable of carrying applied loads. With a focus on large actuated structures, we consider infinite plates of the kind shown in Fig. 2 where the truss part of the structure is comprised of identical repeating units. The effects of finiteness are discussed elsewhere. The first step considers infinite planar trusses with pinned joints.

2.1. Static and kinematic determinacy of infinite planar trusses with repeating units

Maxwell's necessary condition for static determinacy of a pin-jointed truss requires that the number of member forces equal the number of joint equilibrium equations. For an infinite planar truss, this criterion requires an average of four members converging at each joint. Note that the Kagome truss (Fig. 1) satisfies this condition, whereas a triangulated truss with repeating equilateral triangles has an excess of two members at each joint.

Kinematic determinacy for a truss satisfying the above condition requires that joint positions are uniquely determined by member lengths (no mechanisms) such that member lengths can be varied independently without incurring deformation of any members.

Additional conditions must be imposed to ensure static or kinematic determinacy of an infinite, pin-jointed planar truss. These are discussed by Guest and Hutchinson (2002) and applied to periodic trusses such as the Kagome truss. These authors show that infinite trusses built up from repeating units (planar or three-dimensional) cannot satisfy all of the conditions for both static and kinematic determinacy. That is, any such infinite truss that is statically determinate will necessarily have kinematic mechanisms. Conversely, any infinite truss that is kinematically determinate will have states of self-stress.

2.2. The Kagome planar truss: stiffness and uniform actuation strains

The infinite pin-jointed Kagome truss is neither statically nor kinematically determinate (Wicks, 2002) and yet it is capable of bearing arbitrary overall loads. In contrast, for the case of a finite Kagome truss, it is possible to add additional members to the boundaries in order to make it both statically and kinematically determinate.

Consider the infinite Kagome truss and assume that each member is identical with length, L, cross-sectional area, A, and Young's modulus, E. Further, suppose the truss is loaded at infinity such that the normal and tangential stress resultants per unit length acting on an edge perpendicular to the x_1-direction are (N_{11}, N_{12}); similarly, the stress resultants on an edge perpendicular to the x_2-direction are (N_{21}, N_{22}), where $N_{21} = N_{12}$ and notation standard to plate theory is used. All bars with the same inclination carry identical loads. With three representative members denoted by A, B and C and for the truss orientation shown in Fig. 1, the forces are

$$F_A = (L/\sqrt{3})(3N_{11} - N_{22}), \quad F_B = 2L(N_{22}/\sqrt{3} - N_{12}), \quad F_C = 2L(N_{22}/\sqrt{3} + N_{12}) \tag{1}$$

The overall stiffness of the Kagome planar truss is isotropic such that the relation between the average in-plane strains and the overall stress resultants are given by

$$\varepsilon_{11} = S^{-1}(N_{11} - \nu N_{22}), \quad \varepsilon_{22} = S^{-1}(N_{22} - \nu N_{11}), \quad \varepsilon_{12} = S^{-1}(1 + \nu)N_{12} \tag{2}$$

with $S = EA/(\sqrt{3}L)$ and $v = 1/3$. The inverted relation is (with $v = 1/3$)

$$N_{11} = \frac{9}{8}S\left(\varepsilon_{11} + \frac{1}{3}\varepsilon_{22}\right), \quad N_{22} = \frac{9}{8}S\left(\varepsilon_{22} + \frac{1}{3}\varepsilon_{11}\right), \quad N_{12} = \frac{3}{4}S\varepsilon_{12} \tag{3}$$

Hyun and Torquato (2002) optimized the topology of infinite, planar isotropic truss-like structures in order to maximize stiffness for a given weight. They used an evolution algorithm coupled to a general plane stress analysis of the structure to arrive at an optimal geometry. The Kagome truss and the triangulated truss were found to be almost identical in stiffness per unit weight. When analyzed within the framework of pin-jointed trusses, the two geometries are precisely equally optimal, attaining the dilute limit of the Hashin and Strickman (1962) upper bounds.

It is an elementary exercise to relate the overall strains, $(\varepsilon_{11}, \varepsilon_{22}, \varepsilon_{12})$ to the actuation strains $(\varepsilon_A, \varepsilon_B, \varepsilon_C)$ of bars A, B and C, respectively. The overall strains can be achieved without inducing any stress in the members by actuating (i.e. elongating or contracting) the three sets of members according to

$$\varepsilon_A = \varepsilon_{11}, \quad \varepsilon_B = \frac{1}{4}\varepsilon_{11} + \frac{3}{4}\varepsilon_{22} - \frac{\sqrt{3}}{2}\varepsilon_{12}, \quad \varepsilon_C = \frac{1}{4}\varepsilon_{11} + \frac{3}{4}\varepsilon_{22} + \frac{\sqrt{3}}{2}\varepsilon_{12} \tag{4}$$

or

$$\varepsilon_{11} = \varepsilon_A, \quad \varepsilon_{22} = -\frac{1}{3}\varepsilon_A + \frac{2}{3}(\varepsilon_B + \varepsilon_C), \quad \varepsilon_{12} = \frac{1}{\sqrt{3}}(\varepsilon_C - \varepsilon_B) \tag{5}$$

When the joints are welded, bending in the members results in a small resistance to actuation. To estimate the magnitude, note that the strains induced by bending are of order, $(r/L)\varepsilon_A$, where ε_A is taken to be representative the actuation strain and $r = \sqrt{I/A}$ is the radius of gyration of the member, with I as the moment of inertia. Consequently, the elastic energy induced by actuation scales with $E(r\varepsilon_A/L)^2$ multiplied by the volume of truss deformed. The corresponding elastic energy-scaling factor for an actuated redundant truss is $E\varepsilon_A^2$. Thus, the energy stored in actuation of the Kagome truss is expected to be significantly lower than that in a redundant truss.

3. Mechanisms of the planar Kagome pin-jointed structure

It is instructive to determine the full set of possible collapse mechanisms for a pin-jointed planar Kagome structure of infinite extent. A systematic method has been developed to determine the competing collapse mechanisms for any pin-jointed periodic structure (Hutchinson and Fleck, 2002). The method builds upon the matrix methods of structural analysis pioneered by Pellegrino and Calladine (1986) and Pellegrino (1993), and the Bloch wave analysis for periodic continue by Triantafyllidis and Schnaidt (1993). An equivalent approach is to set up the governing set of finite difference equations for a periodic structure (e.g. Forman and Hutchinson, 1970). The main steps in the analysis are as follows:

(i) The kinematic matrix for the unit cell is derived; this relates the bar elongations to the nodal displacements for all nodes and bars of the unit cell.

(ii) For the given unit cell, the trial displacement field d_j^n of each node n at position $\boldsymbol{x}$ is written as

$$d_j^n = p_j^n \exp(\mathrm{i}2\pi\boldsymbol{k}\cdot\boldsymbol{x}) \quad j = 1, 2 \tag{6}$$

The harmonic function $\exp(\mathrm{i}2\pi\boldsymbol{k}\cdot\boldsymbol{x})$ with wavevector $\boldsymbol{k}$, is modulated by an unknown periodic function p_j^n that repeats from one unit cell to the next. Substitution of the trial field (6) into the kinematic matrix for the unit cell leads to a reduced kinematic matrix for the unknown quantities p_j^n for the boundary and interior nodes.

(iii) The possible collapse mechanisms are obtained by taking the bar elongations of the unit cell to equal zero, and by examining the null space of the reduced kinematic matrix for any chosen values of $\boldsymbol{k}$. The dimension of the null space equals the number of mechanisms for the assumed wavevector $\boldsymbol{k}$. In general, the null space is complex, and the real and imaginary parts of the displacement field d_j^n constitute independent mechanisms.

3.1. Application of matrix analysis to the planar Kagome pin-jointed structure

The full set of mechanisms for the pin-jointed planar Kagome structure have been calculated using the above matrix analysis. The Kagome structure is represented by the primitive unit cell as outlined by dotted lines in Fig. 1, with the local co-ordinates $(\hat{x}_1, \hat{x}_2)$ aligned with the sides of the unit cell, and oriented with respect to the Cartesian reference frame (x_1, x_2). Symmetry dictates the existence of three families of collapse mechanism, with one family characterized by the wavevector $\boldsymbol{k}$ along the $\hat{x}_1$-direction, one along the $\hat{x}_2$-direction and the third along the x_2-direction. It suffices to consider the canonical family of mechanisms associated with wavevectors along the x_2-direction; the other two families can be obtained simply by rotating the Kagome structure with its canonical family of mechanisms by a clockwise or counter-clockwise rotation through 60°.

The canonical mechanisms are associated with $|\boldsymbol{k}|$ adopting the following values: $|\boldsymbol{k}| = \sqrt{3}/4L$, $\sqrt{3}/6L$, $\sqrt{3}/8L$, $\sqrt{3}/10L \ldots, 0$. For $|\boldsymbol{k}| = 0$, a single mechanism exists, and it can be characterized by the relative rotation of neighboring triangles, see Fig. 3a. This infinitesimal mechanism does not generate macroscopic strain, but the finite version of this mechanism does give rise to an equi-biaxial compressive strain. The mechanism for $|\boldsymbol{k}| = \sqrt{3}/4L$ resembles twinning of alternating sign along the x_2-direction, as sketched in Fig. 3b. For intermediate values of $|\boldsymbol{k}|$, such as $\sqrt{3}/6L$, two independent collapse mechanisms exist (given by the real and imaginary parts of d_j^n); each collapse mechanism comprises discrete bands of deformation that are periodic along the x_2-direction. For the sake of brevity, these additional collapse mechanisms are not shown, and the reader is referred to Hutchinson and Fleck (2002) for full details.

None of the infinitesimal collapse modes described above gives rise to macroscopic strain. This is consistent with the fact that the Kagome structure has a finite overall stiffness, as given by Eq. (3).

4. Strength of the planar Kagome structure with welded joints

When the joints of the Kagome planar truss are welded, the kinematic mechanisms identified above are suppressed. However, the issue remains as to whether the welded truss is susceptible to buckling in modes of similar shape to the mechanisms described above. This possibility is examined by performing a general

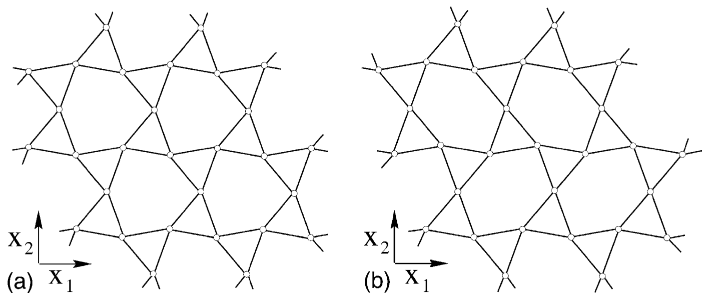

Fig. 3. Mechanisms of the planar Kagome truss. (a) $|\boldsymbol{k}| = 0$ and (b) $|\boldsymbol{k}| = \sqrt{3}/4L$.

bifurcation buckling analysis of the in-plane modes. As in the earlier sections, the length of each member is L, the modulus is E and the cross-sectional area is A. The moment of inertia of the members governing in-plane bending is I. We first consider conditions for plastic yielding of the truss and continue with a complete analysis of the in-plane elastic buckling modes.

4.1. Yield

It is straightforward to obtain analytic expressions for the plastic collapse strength of the Kagome truss by assuming that each member behaves in rigid-ideally plastic manner, with a yield strength σ_Y, and by neglecting the small effect of bending. The effective yield locus is found by setting the bar tensions defined in (1) equal to the fully plastic axial yield load $\pm A\sigma_Y$ with the following results:

$$\begin{aligned} N_{11} - N_{22}/3 &= \pm A\sigma_Y/(\sqrt{3}L) \\ N_{22} - \sqrt{3}N_{12} &= \pm\sqrt{3}A\sigma_Y/(2L) \\ N_{22} + \sqrt{3}N_{12} &= \pm\sqrt{3}A\sigma_Y/(2L) \end{aligned} \tag{7}$$

Note the special case with $N_{12} = 0$ defines a four-sided convex yield locus in the (N_{11}, N_{22}) plane as shown in Fig. 4. The relations (7) can be re-phrased in terms of the principal in-plane stresses (N_1, N_2) and the orientation of the principal directions with respect to the Kagome truss. Using this approach it can be shown that the Kagome truss is almost isotropic in its yield response (Hutchinson and Fleck, 2002).

4.2. Elastic buckling of the Kagome truss

Bloch wave theory can be used to obtain the elastic buckling strength of the welded Kagome truss subjected to arbitrary, macroscopic in-plane loading. Following Triantafyllidis and Schnaidt (1993), the first step is to determine the tangential stiffness matrix $\boldsymbol{K}$ for the primitive unit cell (Fig. 1) at a given macroscopic stress. Let $\boldsymbol{d}$ be the vector of virtual nodal displacements (two translations and one rotation per node), and $\boldsymbol{f}$ be the work-conjugate vector of generalised forces (two direct forces and one moment per node). Then, a non-trivial solution is sought for the homogeneous system of equations $\boldsymbol{Kd} = \boldsymbol{f}$ where $\boldsymbol{K}$ is the symmetric, tangential stiffness matrix of the primitive unit cell, in accordance with beam-column theory (see e.g. Livesley, 1975). One first forms the 15×15 matrix $\boldsymbol{K}$ for the Kagome unit cell of Fig. 1 (five nodes each with three degrees of freedom, d.o.f.) with the axial bar forces determined by the macroscopic stress state using (1). Next, the generalised virtual displacement and force vectors $\boldsymbol{d}$ and $\boldsymbol{f}$ are given a Bloch wave representation similar to (6), and one thereby obtains a (9×9) reduced stiffness matrix $\boldsymbol{K}_r$. The governing equation for any buckling mode now reads $\boldsymbol{K}_r\boldsymbol{d}_r = \boldsymbol{0}$. Further reductions may be made if desired: e.g. one may "statically condense" internal d.o.f. such as those associated with joint 1 in Fig. 1. It is emphasized that the reduced stiffness matrix is a non-linear function of both the assumed pre-buckling stress state and the wavevector $\boldsymbol{k}$.

The buckling load of the welded Kagome truss is obtained by incrementing the macroscopic stress state (and thus the bar forces) along a given stress path, and by searching for a non-trivial solution of $\boldsymbol{K}_r\boldsymbol{d}_r = \boldsymbol{0}$ for all $\boldsymbol{k}$. This null space contains infinitesimal elastic buckling modes (in general, real and imaginary) analogous to the linear eigenvalue buckling analysis found in many commercial finite element codes (e.g. ABAQUS). At low loads the nullspace is trivial whereas at sufficiently high loads buckling is triggered and the nullspace is non-trivial.

The elastic buckling locus in the macroscopic (N_{11}, N_{22}) plane is shown in Fig. 4 for various strut slenderness ratios. In this plot the stress resultants have been normalized by $A\sigma_Y/L$, and, thus, the elastic buckling locus depends upon the magnitude of the yield strain, $\varepsilon_Y = \sigma_Y/E$. Whether elastic buckling or plastic collapse controls the in-plane strength of the truss depends upon the ratio $r/(L\sqrt{\varepsilon_Y})$, where

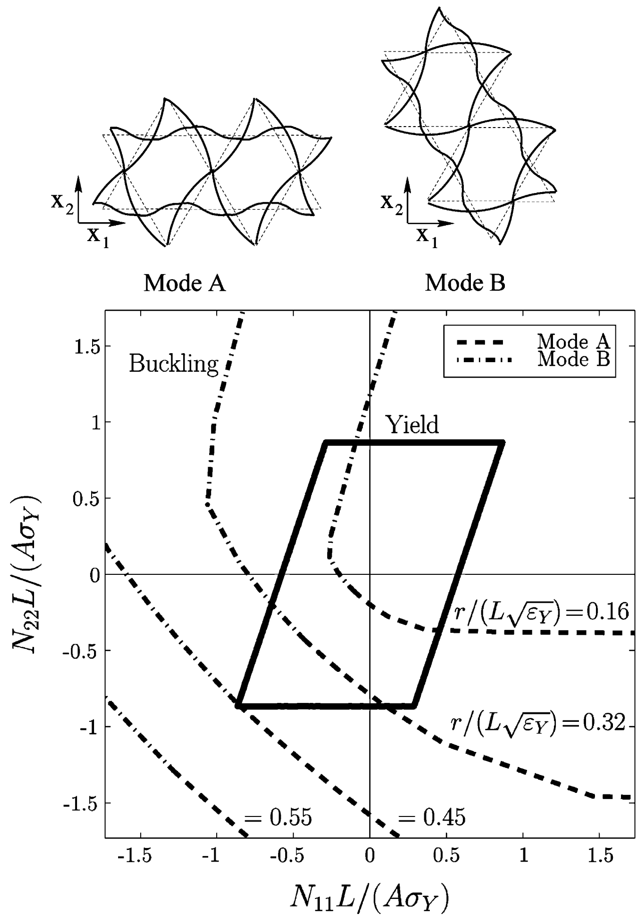

Fig. 4. The competition between elastic buckling and plastic collapse of the welded Kagome truss for selected values of slenderness ratio $r/(L\sqrt{\varepsilon_Y})$.

$r \equiv \sqrt{I/A}$ is the radius of gyration of the cross-section. If $r/(L\sqrt{\varepsilon_Y}) > 0.45$, plastic yielding occurs prior to elastic bucking for all combinations of N_{11} and N_{22}. For example, if $\varepsilon_Y = 0.003$ then plastic yielding is operative if $r/L > 0.024$. In other words, only when its members are exceptionally slender will the weld-jointed Kagome truss be susceptible to elastic buckling.

In general, only two elastic buckling modes—modes A and B (Fig. 4)—are found to be of practical interest; all others occurred at higher loads. Mode A is associated with N_{22}-compression and the wavevector $|\boldsymbol{k}| = \sqrt{3}/4L$ (note similarity to Fig. 3b) while Mode B is associated with N_{11}-compression and is equivalent to Mode A rotated by 60° analogous to the above "canonical pin-jointed mechanism" discussion.

5. Two Kagome sandwich plates

The two sandwich plates considered in this paper are shown in Fig. 2. Actuation of members of the Kagome planar trusses is envisioned. For the plate having just one truss face, it is assumed that face will be actuated to achieve desired shapes of the solid face sheet. The Gaussian curvature of the desired shape must be small, otherwise large actuation forces will be required to overcome stretching of the solid face. For the plate in Fig. 2b with two truss faces, each face will be actuated. This allows arbitrary shapes to be achieved with no restriction on the Gaussian curvature.

For the sandwich plate with a single truss plate, the core is comprised of tetragonal truss units connecting the nodes of the face to the solid face as shown in Fig. 2a. The spacing between the faces is H and the truss face sheet is characterized by (1)–(3). The solid face sheet has Young's modulus, E_f, Poisson's ratio, ν_f, thickness t_f, and stretching stiffness, $S_f = E_f t_f$. The sandwich plate has isotropic stretching and bending stiffnesses that can be readily derived. However, the expressions for these stiffnesses are algebraically lengthy. They simplify significantly if $\nu_f = \nu = 1/3$, in which case the plate stretching stiffness, $\overline{S}$, and bending stiffness, $\overline{B}$, under a single component of moment are given by

$$\overline{S} = S + S_f, \quad \overline{B} = \frac{H^2}{2}\frac{S^2 + S_f^2}{S + S_f} \tag{8}$$

The conventional plate bending stiffness, defined for curvature in only one direction, is $\overline{B}/(1-\nu^2)$.

Second, consider the sandwich plate with two Kagome truss faces; the core comprises tetragonal truss units symmetrically positioned with respect to the mid-plane and connected to the face nodes as shown in Fig. 2b. Eq. (8) applies with S_f denoting the in-plane stiffness of the bottom face. If the two faces are identical, $\overline{S} = 2S$ and $\overline{B} = H^2 S/2$.

6. Long wavelength actuation of Kagome plates

For the plate having one solid face, the Kagome back plane is actuated to achieve the desired shapes (Figs. 2 and 5). For this case, the Gaussian curvature of the goal shape must be small, otherwise large actuation forces will be required to overcome stretching. Conversely, for the plate with two truss faces, both can be actuated to realize arbitrary shapes with no restriction on the Gaussian curvature. The aim is to achieve specified non-planar shapes defined by the transverse displacement field, $w^0(x_1, x_2)$, of the lower face sheet as closely as possible (Fig. 5). When the desired shape has wavelengths that are long compared to the length of the truss members, the analysis is elementary. The results will be presented below. The corresponding analysis for shorter wavelengths will be presented in a subsequent paper.

6.1. Relation between member actuation and average in-plane displacements and strains for long wavelength modes in the two-dimensional Kagome planar truss

Invoke a continuum description of the truss wherein the joints and members are imagined embedded within a planar membrane. Measure displacements and strains from the reference state of the undeformed membrane, and denote them in the usual way for a continuum by $u_\alpha(x_\mu)$ and $\varepsilon_{\alpha\beta} = (u_{\alpha,\beta} + u_{\beta,\alpha})/2$ where the Greek subscripts range from 1 to 2. The displacement of a truss node coincides with the displacement, u_α, of the membrane at that point, and the extensional strain, ε, of a member connecting neighboring nodes I and J is $\varepsilon = (u_\alpha(\vec{x}^I) - u_\alpha(\vec{x}^J))t_\alpha/L$ where t_α is the unit vector parallel to the member and directed from J to I. Equivalently, in the long wavelength limit the member strain can be expressed as $\varepsilon = \varepsilon_{\alpha\beta}t_\alpha t_\beta$ where the strain is evaluated at the member location. Denote the top Kagome face sheet by the superscript T. Then, an

Fig. 5. Desired shape to be achieved by actuation.

arbitrary in-plane displacement field, u^{T}_{α}, of the truss joints can be achieved by actuation of the members to undergo the extensional strain described above and derived from u^{T}_{α}, i.e. $\varepsilon^{\mathrm{T}} = (u^{\mathrm{T}}_{\alpha}(\vec{x}^{I}) - u^{\mathrm{T}}_{\alpha}(\vec{x}^{J}))t_{\alpha}/L$. Thus, the Kagome planar truss can be actuated to achieve any long wavelength, in-plane strain field, $\varepsilon^{\mathrm{T}}_{\alpha\beta} = (u^{\mathrm{T}}_{\alpha,\beta} + u^{\mathrm{T}}_{\beta,\alpha})/2$. Relations (4) and (5) can be used to obtain the member actuation strains from $\varepsilon^{\mathrm{T}}_{\alpha\beta}$. If the Kagome truss plate had true pin joints, arbitrary member actuation would leave the truss unstressed. The welded-joint Kagome truss is capable of arbitrary actuation without substantial resistance, while at the same time being stiff and strong in all directions.

6.2. Actuation of a Kagome-backed truss plate for long wavelength shapes

The combination of qualities noted above make the Kagome truss a unique two-dimensional element for actuating either of the plate structures shown in Fig. 2. The passive bending behavior of each of the plates is isotropic and substantial, as is the stretching stiffness. Moreover, the sandwich plate has a high resistance to local buckling. Under the restriction of long wavelength actuation modes, it will be shown that the Kagome planar truss comprising the top face of the plate can be actuated to achieve any normal deflection shape of the bottom face sheet, provided that the deflection slopes are sufficiently small. As already noted, larger deflections are limited to those shapes for which the Gaussian curvature of the solid face sheet is small. For the plate having a Kagome planar truss for both faces, this restriction can be removed if both faces are actuated, as will be discussed in Section 6.3.

Let $\varepsilon^{0}_{\alpha\beta}$ be the in-plane strains of the virtual middle surface of the sandwich. Let $w^{0}(x_1, x_2)$ be the normal deflection of that surface with $\kappa^{0}_{\alpha\beta}$ as its curvature tensor, where $\kappa^{0}_{\alpha\beta} = w^{0}_{,\alpha\beta}$. With $u^{0}_{\alpha}(x_{\beta})$ as the in-plane displacements of the virtual middle surface, the in-plane strains are given by

$$\varepsilon^{0}_{\alpha\beta} = \tfrac{1}{2}(u^{0}_{\alpha,\beta} + u^{0}_{\beta,\alpha}) + \tfrac{1}{2}w^{0}_{,\alpha}w^{0}_{,\beta} \tag{9}$$

The compatibility equation for the middle surface strains is

$$\varepsilon^{0}_{11,22} + \varepsilon^{0}_{22,11} - 2\varepsilon^{0}_{12,12} = \mathsf{G} \tag{10}$$

where $\mathsf{G} = \kappa^{0^2}_{12} - \kappa^{0}_{11}\kappa^{0}_{22}$ is the Gaussian curvature of the middle surface. The formulation is limited to the same restrictions as von Karman nonlinear plate theory: small strains and moderately large out-of-plane rotations such that $|u^{0}_{,\alpha}| \ll 1$ and $|w^{0}_{,\alpha}|^2 \ll 1$. For a core with ample shear stiffness, the strains in the top and bottom faces can be expressed in terms of the middle surface strain and curvature using the classical Euler–Bernoulli hypothesis. This hypothesis states that material points lying on a normal to the undeformed middle surface remain on the normal to the deformed middle surface. For the top Kagome face this implies

$$\varepsilon^{\mathrm{T}}_{\alpha\beta} = \varepsilon^{0}_{\alpha\beta} - (H/2)\kappa^{0}_{\alpha\beta} \tag{11}$$

while for the bottom face (Kagome or solid)

$$\varepsilon^{B}_{\alpha\beta} = \varepsilon^{0}_{\alpha\beta} + (H/2)\kappa^{0}_{\alpha\beta} \tag{12}$$

Let $w^{0}(x_1, x_2)$ be the desired shape of the plate. (Under the present restrictions for which (11) and (12) apply, both the top and bottom face sheets have the same normal deflection as the virtual middle surface.) The objective is to activate the top Kagome truss sheet to achieve $w^{0}(x_1, x_2)$ such that there is no stretching strain in the bottom face sheet. This ensures that any resistance to actuation is due only to bending and, therefore, relatively small. Imposing $\varepsilon^{B}_{\alpha\beta} = 0$, requires $\varepsilon^{0}_{\alpha\beta} = -(H/2)\kappa^{0}_{\alpha\beta}$. Then, by (11), it follows that the top Kagome truss sheet must be activated such that $\varepsilon^{\mathrm{T}}_{\alpha\beta} = -H\kappa^{0}_{\alpha\beta}$. Compatibility of the middle surface strains, $\varepsilon^{0}_{\alpha\beta}$, requires that (10) be satisfied. Since $\varepsilon^{0}_{\alpha\beta} = -(H/2)w^{0}_{,\alpha\beta}$ satisfies $\varepsilon^{0}_{11,22} + \varepsilon^{0}_{22,11} - 2\varepsilon^{0}_{12,12} = 0$ identically, it follows from (10) that the choice of shape $w^{0}(x_1, x_2)$ must be restricted to have zero Gaussian curvature, that is

$\mathsf{G} \equiv \kappa_{12}^{0^2} - \kappa_{11}^0\kappa_{22}^0 = w_{,12}^{0^2} - w_{,11}^0 w_{,22}^0 = 0$. (This condition can be relaxed for sufficiently small deflection slopes, as will be discussed later.)

Assuming $\mathsf{G} = 0$, the nodal displacements in the top Kagome truss needed to achieve the strains $\varepsilon_{\alpha\beta}^{\mathrm{T}} = -H\kappa_{\alpha\beta}^0$ are $u_\alpha^{\mathrm{T}} = -Hw_{,\alpha}^0$ and the elongation (or contraction), ΔL, of a member with orientation specified by the unit vector t_α is

$$\Delta L = -HL\kappa_{\alpha\beta}^0 t_\alpha t_\beta \tag{13}$$

As discussed above, this displacement field can always be achieved by actuating members of the Kagome truss plane. Moreover, upon actuating to produce any shape of zero Gaussian curvature there are no induced stresses except those caused by truss bending. Additional loads applied to the sandwich plate induce both bending and stretching. The members and solid face sheet must be designed to carry those loads. The work of actuation is that required to displace the applied loads, plus the small internal energy stored in bending.

The condition on w^0 that $\mathsf{G} = \kappa_{12}^{0^2} - \kappa_{11}^0\kappa_{22}^0 = 0$ ensures that no stretch energy occurs in the face sheets. When the slopes of the desired shape, $w_{,\alpha}^0$, are restricted to be sufficiently small, the Gaussian curvature can be taken to vanish (since it is quadratic in $w_{,\alpha\beta}^0$), and the compatibility equation (10) can be linearized, with its right hand side vanishing identically. Then, *any* shape w^0 can be achieved by actuating the top Kagome truss, but some stretching energy will be induced if $G \neq 0$. The practical limits to the linear regime will depend on energy requirements for actuation and on buckling as well as plastic yielding constraints in the truss members and the solid face sheet.

6.3. Long wavelength actuation of both faces of a two-faced Kagome truss plate

If members of each face of the two-faced Kagome truss plate in Fig. 2 can be actuated, it is possible to achieve arbitrary shapes with no restriction on the Gaussian curvature of the desired shape. Given the desired shape, $w^0(x_1, x_2)$, take $u_\alpha^0 = -(1/2)Hw_{,\alpha}^0$ such that, by (9), $\varepsilon_{\alpha\beta}^0 = -(1/2)Hw_{,\alpha\beta}^0 + (1/2)w_{,\alpha}^0 w_{,\beta}^0$. (This choice necessarily satisfies (10).) Then, by (11) and (12), the strains that must be attained by actuation in the top and bottom faces are $\varepsilon_{\alpha\beta}^{\mathrm{T}} = -H\kappa_{\alpha\beta}^0 + (1/2)w_{,\alpha}^0 w_{,\beta}^0$ and $\varepsilon_{\alpha\beta}^B = (1/2)w_{,\alpha}^0 w_{,\beta}^0$, respectively. These strains are achieved by actuating length changes of the members according to $\Delta L = L\varepsilon_{\alpha\beta}t_\alpha t_\beta$, as already discussed.

It is worth noting that, as specified, the scheme is not unique. To prescribe unique actuation of the members, both the in-plane displacements and the normal deflection must be prescribed. If the virtual mid-plane undergoes displacements (u_α^0, w^0), $\varepsilon_{\alpha\beta}^0$ is given by (9). Then, by (11) and (12), the face sheets must be actuated to achieve (u_α^0, w^0) such that

$$\varepsilon_{\alpha\beta}^{\mathrm{T}} = \tfrac{1}{2}(u_{\alpha,\beta}^0 + u_{\beta,\alpha}^0) - \tfrac{1}{2}H\kappa_{\alpha\beta}^0 + \tfrac{1}{2}w_{,\alpha}^0 w_{,\beta}^0 \quad \text{and} \quad \varepsilon_{\alpha\beta}^B = \tfrac{1}{2}(u_{\alpha,\beta}^0 + u_{\beta,\alpha}^0) + \tfrac{1}{2}H\kappa_{\alpha\beta}^0 + \tfrac{1}{2}w_{,\alpha}^0 w_{,\beta}^0$$

The displacements in the bottom face are $(u_\alpha^0 + (1/2)Hw_{,\alpha}^0, w^0)$. Thus, if the aim is to activate the top and bottom face sheets such that the bottom face sheet undergoes displacements (u_α^B, w^B), this can be achieved without incurring stretching energy by substituting $w^0 = w^B$ and $u_\alpha^0 = u_\alpha^B - (1/2)Hw_{,\alpha}^0$ into the expressions just listed to obtain

$$\varepsilon_{\alpha\beta}^{\mathrm{T}} = \frac{1}{2}(u_{\alpha.\beta}^B + u_{\beta,\alpha}^B) - H\kappa_{\alpha\beta}^B + \frac{1}{2}w_{,\alpha}^B w_{,\beta}^B \quad \text{and} \quad \varepsilon_{\alpha\beta}^B = \frac{1}{2}(u_{\alpha.\beta}^B + u_{\beta,\alpha}^B) + \frac{1}{2}w_{,\alpha}^B w_{,\beta}^B \tag{14}$$

with $\kappa_{\alpha\beta}^B = w_{,\alpha\beta}^B$.

In summary, a plate having actuated Kagome planar trusses for each face can achieve any desired displacement of the nodes of one of the faces, in-plane and out-of-plane. The resistance to actuation is due only to truss bending effects. A prescription for shapes having wavelengths that are long compared to the plate thickness is presented. This prescription applies to shapes with moderately large slopes, $|w_{,\alpha}^0|^2 \ll 1$. It can be extended to shallow shells in a straightforward manner.

7. Concluding remarks

The Kagome truss has been introduced as an actuating plane into a sandwich plate structure with the potential for achieving arbitrary non-planar shapes. The primary feature of the weld-jointed Kagome truss for actuation applications is its ability to deform as an effective medium with arbitrary in-plane strains against the minimal bending resistance of the joints. Other properties that make it especially effective for such applications are its isotropic stiffness, its substantial, near-isotropic in-plane yield strength, and its high local buckling strength. The sandwich plate with two Kagome truss faces can be actuated to achieve arbitrary displacements of the nodes of one face. The plate with only one face as a Kagome truss can be actuated to deform the solid skin to a desired shape. However, unless the Gaussian curvature of the desired shape is small, significant stretching forces will develop and the energy of actuation will be large.

When the actuation is limited to long wavelength modes surprisingly simple results pertain. Methods are being developed to cope with actuation into arbitrary shapes, including a detailed assessment of the stresses produced by both the actuation and by the applied loads to be displaced. Problems related to the potential for fatigue at welded joints will be addressed. More detailed results on the buckling strength will be published separately (Hutchinson and Fleck, 2002). Optimization of plates designed for specific actuation goals will also be performed in subsequent work.

Finally, we note that it has been possible to fabricate the panels described in Fig. 2 by using a procedure based on the CNC bending of perforated plates, followed by transient liquid phase bonding of the faces to the core. Tests on these structures are in progress to affirm the stiffness and strength, to ascertain the bending resistance of welded truss joints, and to establish limits on the realizable deformations imposed by fatigue.

Acknowledgements

This work was supported in part by the ONR Grant: Multifunctional Mechano-Electronic Materials and by Cambridge University, Harvard University and the University of California, Santa Barbara.

References

Forman, S.E., Hutchinson, J.W., 1970. Buckling of reticulated shell structures. Int. J. Solids Struct. 6, 909–932.

Guest, S.D., Hutchinson, J.W., 2002. On the determinacy of repetitive structures. J. Mech. Phys. Solids 51, 383–391.

Hashin, Z., Strickman, S., 1962. On some variational principles in anisotropic and non-homogeneous elasticity. J. Mech. Phys. Solids 10, 335–342.

Hutchinson, R.G., Fleck, N.A., in preparation.

Hyun, S., Torquato, S., 2002. Optimal and manufacturable two-dimensional Kagome-like cellular solid. J. Mater. Res. 17 (1), 137–144.

Livesley, R.K., 1975. Matrix Methods in Structural Analysis, second ed. Pergamon Press.

Mikulas, M.M., Thorwald, G., Wada, B.K., 1993. Design considerations for doubly curved conformable trusses. Report JPL D-10528, Jet Propulsion Lab, Caltech, Pasadena, CA.

Miura, K., 1984a. Design and operation of a deployable truss structure. In: Proceedings of 18th Aerospace Mechanisms Symposium, 2–4 May 1984, NASA Goddard Space Flight Center, Greenbelt, Maryland, NASA-CP-2311. pp. 49–63.

Miura, K., 1984b. Variable geometry truss and its application to deployable truss and space crane arm. In: Proceedings of 35th Congress of the International Astronautical Federation, 7–13 October 1984, Lausanne, Switzerland, IAF-84-394.

Pellegrino, S., 1993. Structural computations with the singular value decomposition of the equilibrium matrix. Int. J. Solids. Struct. 30, 3025–3035.

Pellegrino, S., Calladine, C.R., 1986. Matrix analysis of statically and kinematically indeterminate frameworks. Int. J. Solids. Struct. 22, 409–428.

Rhodes, M.D., Mikulas, M.M., 1985. Deployable controllable geometry truss beam. NASA Langley Research Center Report, NASA TM-86366.

Triantafyllidis, N., Schnaidt, W.C., 1993. Comparison of microscopic and macroscopic instabilities in a class of two-dimensional periodic composites. J. Mech. Phys. Solids 41, 1533–1565.

Wicks, N., 2002. Optimization and actuation of truss structures, in preparation.